UDC 621.694:533.697.5 **doi: 10.20998/2411-3441.2023.2.02**

A. ROGOVYI, REN QINGSHENG, WANG XINGRONG, A. NESKOROZHENYI, Y. TIMCHENKO

IMPROVEMENT OF DIMENSIONS AND CHARACTERISTICS OF THE VORTEX CHAMBER PUMP FOR COAL-WATER MEDIUM DELIVERING

The vortex chamber pump combines the positive characteristics of the centrifugal pump and the jet pump, and its efficiency is much higher than that of the classical jet pump. This pump differs from the vortex injector by having the pump flow into the tangential outlet channel, which is not available in the vortex injector. The traditional bulk material pump in many aspects has certain shortcomings, these shortcomings limit its application scope and use effect, the traditional bulk material pumps mechanical parts and seals rapidly wear, resulting in short service life. Based on solving the Reynolds equations for water flow, the influence of the angle between the tangential channels of the pump on the energy characteristics is analyzed: an increase in the angle to 180° leads to a decrease in the relative efficiency by 30 %, the outlet pressure by 12 %, and the suction flow rate by 14 %. Thus, the design with a zero angle between the tangential active medium inlet and the tangential outlet channels is optimal in terms of energy-saving pumping performance. As the diameter of the vortex chamber increases, there is no significant trend in the efficiency of the pumped fluid be the vortex chamber pump. With the increase in the total supply pressure, the axial inlet flow rate increase is relatively slow, and the outlet flow rate increases in a parabolic trend. The wear of the pump vortex chamber wall depends on the mass flow rate of coal entering the vortex chamber. The larger the mass flow rate of the abrasive medium, the greater the erosion rate density and the mean volume fraction in the vortex chamber of the vortex chamber pump. The smaller the particle diameter of the coal, the larger the erosion rate density and mean volume fraction in the vortex chamber of the vortex chamber pump. Thus, an increase in particle size should be sought, which will result in less wear.

Keywords: vortex chamber pump, mathematical modelling, wear, coal, water.

А. С. РОГОВИЙ, РЕНЬ ЦІНШЕН, ВАН СІНРУН, А. О. НЕСКОРОЖЕНИЙ, Є. І. ТІМЧЕНКО

УДОСКОНАЛЕННЯ ГЕОМЕТРИЧНИХ РОЗМІРІВ І ХАРАКТЕРИСТИК ВИХОРОКАМЕРНИХ НАСОСІВ ДЛЯ ПЕРЕКАЧУВАННЯ ВОДОВУГІЛЬНОГО СЕРЕДОВИЩА

Вихорокамерний насос поєднує в собі позитивні характеристики відцентрового і струминного насосів, а його ефективність набагато вища, ніж у класичного струминного насоса. Цей насос відрізняється від вихрового ежектора тим, що потік подається в тангенціальний вихідний канал, який відсутній у вихровому інжекторі. Традиційний насос для сипучих матеріалів у багатьох аспектах має певні недоліки, ці недоліки обмежують сферу його застосування, механічні деталі та ущільнення традиційних насосів для сипучих матеріалів швидко зношуються, що призводить до короткого терміну служби. На основі розв'язання рівнянь Рейнольдса для потоку води проаналізовано вплив кута між тангенціальними каналами насоса на енергетичні характеристики: збільшення кута до 180° призводить до зменшення відносного ККД на 30 %, тиску на виході – на 12 %, а витрати всмоктування – на 14 %. Таким чином, конструкція з нульовим кутом між тангенціальним входом активного середовища і тангенціальним вихідним каналами є оптимальною з точки зору енергозберігаючих характеристик насоса. Зі збільшенням діаметра вихрової камери не спостерігається суттєвої тенденції до зниження ефективності перекачування рідини насосом. Зі збільшенням загального тиску подачі осьова витрата на вході збільшується відносно повільно, а витрата змішаного потоку на виході зростає за параболічним трендом. Знос стінки вихрової камери насоса залежить від масової витрати вугілля, що надходить у вихрову камеру. Чим більша масова витрата абразивного середовища, тим більша щільність швидкості ерозії і середня об'ємна частка твердого сипучого середовища у вихровій камері насоса. Чим менший діаметр частинок вугілля, тим більша щільність швидкості ерозії і середня об'ємна частка у вихровій камері насоса. Таким чином, слід прагнути до збільшення розміру частинок, що призведе до меншого зносу.

Ключові слова: вихорокамерний насос, математичне моделювання, зношування, вугілля, вода.

Introduction. In many industries, traditional pumps delivering bulk materials have some disadvantages in many aspects, including frequent maintenance, high failure rate, high cost, limited transmission distance, limited lift, requiring a large amount of water, and having a great impact on environmental shadow [1]. The failure rate of traditional bulk material pumps is high, because in the production and operation of the pump, various factors such as material quality, processing accuracy, installation and debugging, and maintenance will have an impact on the performance and life of the pump. In addition, the operating environment of the pump can also affect its failure rate, such as shock stress, vibration, chemical corrosion, and heat. Thus, in the pumping of bulk materials, shock stress, vibration, chemical corrosion, and high heat requirements, the reliability of the pump is especially important, the traditional bulk material pump in many aspects has certain shortcomings, and these shortcomings limit its application scope and use effect, the traditional bulk material pump mechanical parts and seals rapid wear, resulting in short service life [2].

Literature review. Classic pumps are prone to rapid grinding wear due to the use of mechanical moving parts and seals. Practically all pump units used in hydraulic conveying plants, except for jet pump units, are subject to considerable wear and tear, as a result of which the average MTBF of pumps and parts varies between 700–2000 hours. In addition, increasing the service life requires the use of more expensive materials that are less susceptible to corrosion and abrasion [3, 4]. Improving the performance of the pumping bulk material device is an urgent problem to be solved [5]. In the papers [6–8] the new jet pump, the vortex chamber supercharger (VCS), is shown (Fig. 1). If the liquid is pumped, then the supercharger can be called a vortex chamber pump (VCP). The VCP can move solid particles in comparison with vortex ejectors which cannot do it because they have an axial exit channel [9, 10]. Moreover, the efficiency of the VCP is higher. Thus, further improvement of jet superchargers, and search for new technical solutions based on more efficient principles of energy transfer will allow to reduce specific energy consumption and improve economic characteristics of hydrotransportation.

In the previous studied was created the vortex

chamber supercharger with proper geometrical dimensions for delivering air with solid particles in pneumatic transport [1, 7, 8]. But VCS needs to be verified for delivering water and also it needs to optimize the angle between tangential channels and the diameter of the vortex chamber.

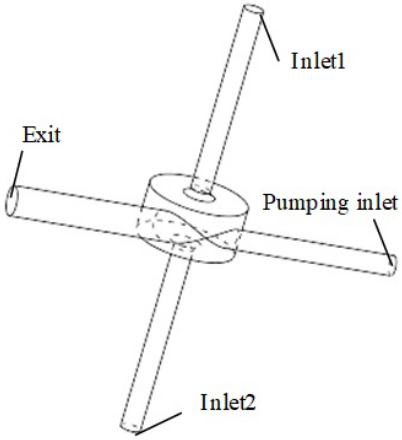

Fig 1. Vortex chamber pump layout

In addition, the pumping of coal particles can result in significant concentrations of coal particles, which can result in significant wear on the vortex chamber [11]. Therefore, it is necessary to estimate the concentrations of solids during pumping and to estimate the wear [12].

Goal. This work aims to improve the performance of the vortex chamber pump when pumping water, to optimize the angle between tangential channels and the diameter of the vortex chamber, to establish patterns of coal particulate flow in water, and to determine the wear characteristics of the vortex chamber.

Research Methodology. This study was carried out in two stages. First, a numerical simulation of the water flow in the vortex chamber pump was carried out based on the solution of the RANS (Reynolds-averaged Navier-Stokes equations) [13] using the Shear stress transport (SST) turbulence model [14]:

$$\frac{\partial u_i}{\partial t}+u_j\frac{\partial u_i}{\partial x_j}=F_i-\frac{1}{\rho}\frac{\partial p}{\partial x_i}+\frac{\partial}{\partial x_j}\left[\frac{\mu_{ef}}{\rho}\frac{\partial u_i}{\partial x_j}\right];\quad \frac{\partial u_i}{\partial x_i}=0;$$

$$\frac{\partial(\rho k)}{\partial t}+\frac{\partial}{\partial x_j}\left(\rho u_j k\right)=\frac{\partial}{\partial x_j}\left(\mu_{ef}\frac{\partial k}{\partial x_j}\right)+P_k-\beta^*\rho k\omega;$$

$$\frac{\partial(\rho\omega)}{\partial t}+\frac{\partial}{\partial x_j}\left(\rho u_j\omega\right)=\frac{\partial}{\partial x_j}\left(\mu_{ef}\frac{\partial\omega}{\partial x_j}\right)-\rho\beta\omega^2+$$

$$+Cd_\omega+\alpha\frac{\rho}{\mu_t}P_k,$$

where x_j are coordinates; u_j are the velocity vector components; ρ is the density; $\mu_{ef}=\mu+\mu_t$ is the effective viscosity; μ_t is the turbulent viscosity; μ is the molecular viscosity; k is the kinetic energy of the turbulence pulsation; ω is the turbulence eddy frequency; Cd_ω is the cross-diffusion term in the SST-model; P_k is the production of turbulence kinetic energy.

The empirical function for sensitization of the SST model to the effects of streamline curvature and system rotation is defined by:

$$f_{r_1}=\max\left\{\min\left(f_{rotation},1.25\right),0.0\right\},$$

where

$$f_{rotation}=(1+c_{r1})\frac{2r^*}{1+r^*}\left[1-c_{r3}\tan^{-1}\left(c_{r2}\tilde{r}\right)\right]-c_{r1},$$

$$c_{r1}=1,\quad c_{r2}=2,\ c_{r3}=1;$$

$$r^*=\frac{S}{\Omega},\ \tilde{r}=2\Omega_{ik}S_{ik}\left[\frac{DS_{ij}}{Dt}+\left(\varepsilon_{imn}S_{jn}+\varepsilon_{jmn}S_{in}\right)\Omega_m^{rot}\right]\frac{1}{\Omega D^3},$$

$$S_{ij}=\frac{1}{2}\left(\frac{\partial u_i}{\partial x_j}+\frac{\partial u_j}{\partial x_i}\right);$$

$$\Omega_{ij}=\frac{1}{2}\left(\left(\frac{\partial u_i}{\partial x_j}-\frac{\partial u_j}{\partial x_i}\right)+2\varepsilon_{mji}\Omega_m^{rot}\right);$$

$$S^2=2S_{ij}S_{ij};\quad \Omega^2=2\Omega_{ij}\Omega_{ij};\quad D^2=\max\left(S^2,0.09\omega^2\right).$$

The simulation was carried out in the commercial software Ansys CFX with the student license. The tetragonal grids were used [15, 16]. The sensitivity of the solution to the mesh size was determined. The convergence of the numerical model was tested based on the achievement of all the residuals up to values of 10^{-5}, as well as the independence of the flow rates in the pump channels from iterations [17].

After carrying out calculations in water, the trajectories of anthracite particles and their flow rates in the suction channels and in the outlet channel of the mixed flow were determined [18]. For the dispersed phase, the anthracite particle trajectory is calculated by integrating the force balance. It was considered that solid particles have a spherical form. Furthermore, all particles are treated as point masses by the CFD code so that an equation for the torque is omitted [19]:

$$\frac{d\vec{V}_p}{dt}=\vec{F}_D+\vec{F}_P,$$

where $\vec{F}_D$, $\vec{F}_P$ represent the drag force and the pressure gradient force, the expressions of which are given as:

$$\vec{F}_D=\frac{3\mu}{4\rho_p d_p^2}C_D\,\mathrm{Re}_s\left(\vec{u}-\vec{V}_p\right);$$

$$\vec{F}_P=\left(\frac{\rho}{\rho_p}\right)\nabla p,$$

where C_D is the drag coefficient [20]:

$$C_D=\begin{cases}\dfrac{24}{\mathrm{Re}_p}\left(1+\dfrac{1}{18}\mathrm{Re}_p^2\right); & \mathrm{Re}_p\le 1000;\\ 0.424; & \mathrm{Re}_p>1000.\end{cases}$$

Re_p is the particle Reynolds number, $Re_p = \rho d_p \left|\vec{V}_p - \vec{u}\right| / \mu$, V_p is the particle velocity, d_p is the particle diameter, ρ_p is the density of particles.

The adequacy of the mathematical model of the flow in the vortex chamber pump was verified by experimental data. The discrepancy did not exceed 10 %.

Results. The vortex chamber pump generally consists of a cylindrical vortex chamber, two axisymmetric axial channels and two tangential channels (Fig. 1, 2). The main parameters of the vortex chamber pump are given in Table 1 below.

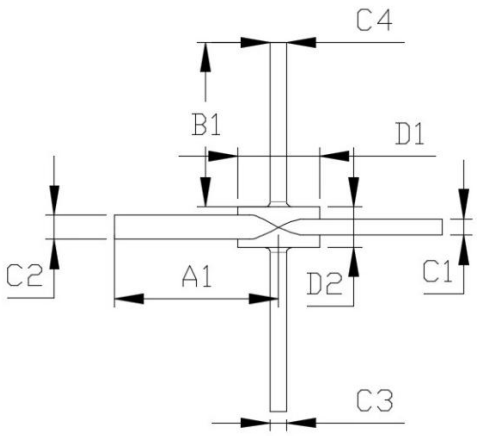

Fig. 2. Main dimensions of the VCP

Table 1 – Main parameters of vortex chamber pump

Dimensions	VCP
Tangential channel length A1/mm	100
Axial channel B1/mm	100
Tangential inlet diameter C1/mm	10
Tangential outlet diameter C2/mm	15
Axial inlet C3/mm	10
Axial inlet C4/mm	10
Vortex chamber diameter D1/mm	50
Vortex chamber height D2/mm	30

The general mesh template of the Ansys Meshing was used to generate the tetrahedral mesh for the VCP. Curvature Normal Angle is set to 11°, Min Size adopts the default value of mesh generation of $1.54 \cdot 10^{-4}$ m, the minimum edge length of the mesh is $3.15 \cdot 10^{-2}$ m, Transition Ratio is set to 0.77, Maximum Layers is set to 5, Growth Rate is set to 1.2. After the system automatically generates the mesh, the number of mesh elements of the vortex chamber supercharger is 302, 117, and the mesh refinement is carried out in the connections and edges of the model in order to ensure the readiness of the calculation.

The grid convergence analysis is carried out before the model calculation run to ensure that the model division grid will not affect the results of the model calculation. For the format analysis of the mesh, the density of the grid has a great impact on the run convergence and stability characteristics, to carry out the grid irrelevance verification, while ensuring that the other boundary conditions remain unchanged at the same time divided into 10 kinds of sparsity of different degrees of mesh. The VCP model had grids with 12000, 20000, 30000, 42000, 52000, 62000, 71000, 83000, 92000, and 110000. The curves shown in Fig. 3 were plotted according to the numerical simulation of the outlet flow rate results of the fluid pumped by the VCP as a reference basis. The results show that when the number of grid elements is not less than 92000, the flow rate at the outlet of the VCP tends to stabilize, indicating that the calculation results will not change significantly, indicating that the grid setting of the model satisfies the calculation of the operational results. Based on not less than the minimum number of mesh elements, the default number of mesh elements generated by the system is selected as 300000, which is used as the final calculation model of the pump.

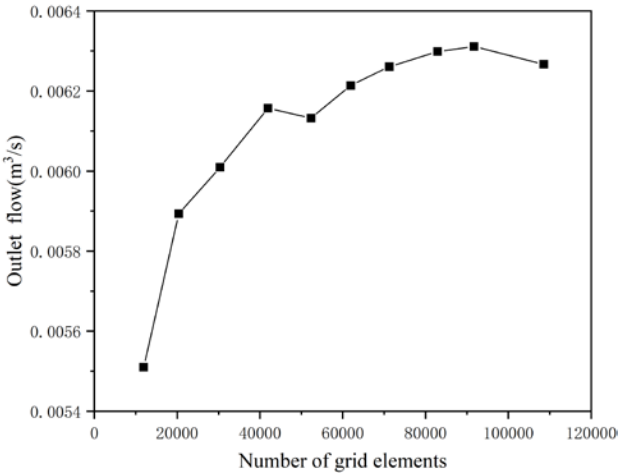

Fig. 3. Grid independence verification

The boundary conditions for water flow are presented in Fig. 4.

The characteristics of the pumping water are the relationship between the relative pressure and efficiency of the device outlet, as well as the relative suction rate (the so-called ejection coefficient, entertainment ratio) of the relative mass flow rate entering the device from the inlet. All features of VCP can be simplified into a universal feature $p = f(m)$, as well as other types of turbochargers.

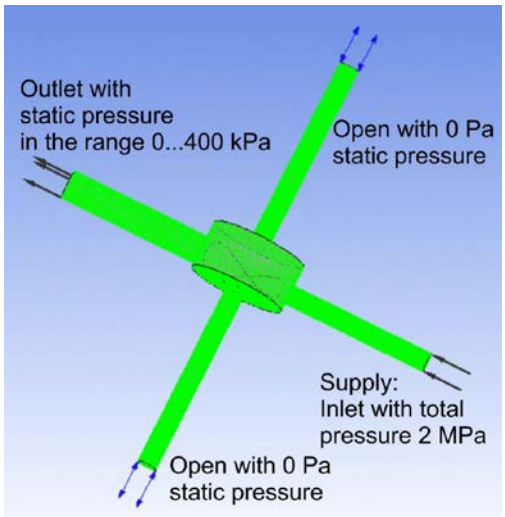

Fig. 4. The boundary conditions for pumping the water

From Fig. 5, it can be seen that the efficiency is highest in the region of 1.36 m_e/m_s. As the ratio p_e/p_s increases, the ratio of m_{in}/m_s decreases. Here, $m_{in} = m_{in1} + m_{in2}$. Here m_e is the outlet mass flow rate, m_s is the supply flow rate, p_e is the static pressure at the outlet, p_s is the static supply pressure, m_{in1}, m_{in2} are the mass flow rates in axial channels.

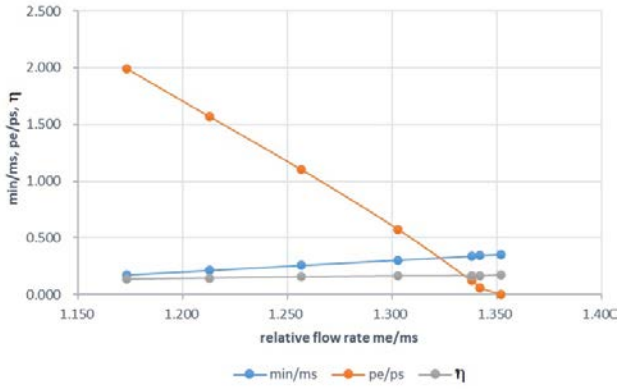

Fig. 5. Calculated characteristics for water delivering

To optimize the angle between the tangential channels, three models of the supercharger were prepared with angles of 0, 90, and 180º (Fig. 6). To simplify the comparison of results, the integral indicators (efficiency, suction flow through the axial channels, and outlet pressure in the tangential channel) are referred to the characteristics of the basic design with a zero angle between the channels.

a *b* *c*

Fig. 6. The computational model of the VCP:
a – the angle between the tangential channels of Supply and Exit is 0°; *b* – the angle is 90°; *c* – the angle is 180°

Fig. 7 and 8 show a comparison of water pumping efficiency at different angles between the tangential channels. The optimal angle for a structure without a drainage channel is 0º. This is because most of the energy of the main flow goes directly into the tangential outlet channel without losses during movement and friction against the walls of the vortex chamber.

The fluid streamlines in the VCP with different angles between channels are presented Fig. 9 and 10.

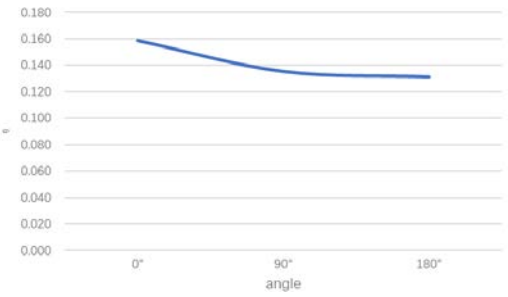

Fig. 7. Efficiency of the different channel positions

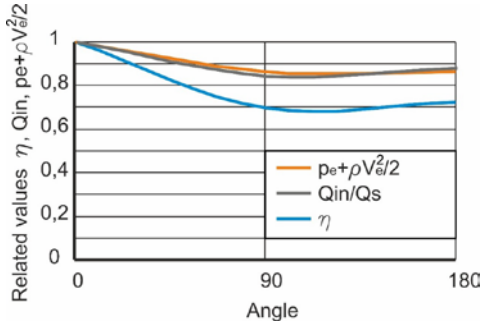

Fig. 8. Related values of the different channel positions

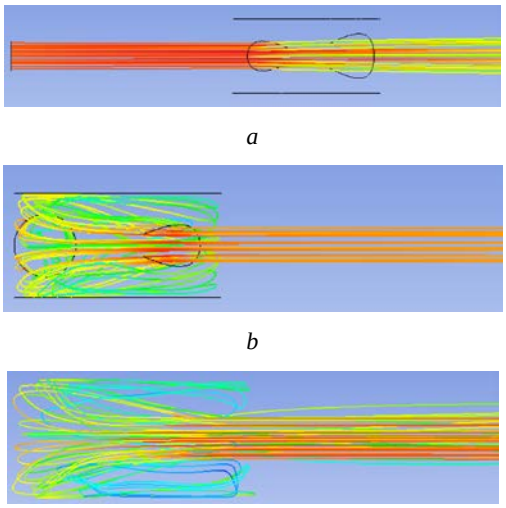

a

b

c

Fig. 9. Streamlines in the meridional plane of the VCP:
a – 0°; *b* – 90°; *c* – 180°

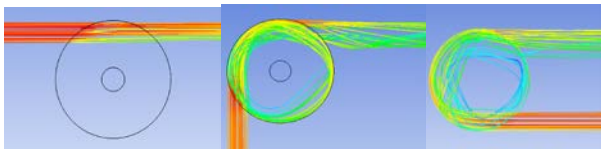

a *b* *c*

Fig. 10. Streamlines in the VCP:
a – 0°; *b* – 90°; *c* – 180°

To objectively analyze the fluid motion characteristics of the VCP, analyze the change rule of outlet and axial inlet flow rates under different energy supplies, respectively set the total pumping inlet pressure of 2 MPa, 4 MPa, 6 MPa, 8 MPa, 10 MPa. As shown in Fig. 11, with the increase in the total supply pressure, the axial inlet flow rate increase is relatively slow, and the outlet flow rate increases in a parabolic trend.

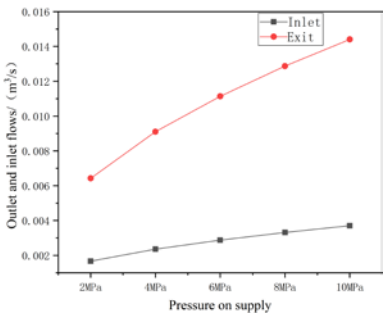

Fig. 11. Fluid flow curves for different supply pressures

To further analyze the effect of pressure on characteristics, analyze the VCP of different pressures of the change rule of efficiency. The results show that the efficiency is in the range of fluctuations between 17.6 % and 17.8 %, the pressure value of the changes in the efficiency is not very obvious. When the pressure continues to increase to 10 MPa there is a trend of decreasing efficiency. This is consistent with the increase in pressure inlet and outlet flow rate increases slowly, indicating that with the increasing pressure VCP efficiency not only cannot increase at the same time, but there will be a tendency to reduce.

The VCP has a good conveying effect for bulk materials, but the efficiency of pumping water has not been significantly improved. The working principle of VCP pressurization is to form a pressure difference between the circumferential and axial areas of the vortex chamber through the movement of the fluid inside the vortex chamber. The channels on both sides of the axial direction are in the low-pressure area, causing it to pump fluid. When the fluid enters the vortex chamber and moves with the internal rotating fluid, the fluid generates additional centrifugal force during the rotating motion, increasing the velocity of the fluid and jetting it out along the tangential outlet of the vortex chamber, thus completing the function of pumping the fluid. The working efficiency of VCP is mainly influenced by the flow rate of axial suction fluid and the magnitude of the additional centrifugal force of the fluid. To increase the transmission efficiency of VCP-pumped fluid and explore the influence of the VCP mechanism on its efficiency, an optimization design is now carried out for the diameter of the vortex chamber. The diameter of the prototype vortex chamber was 50 mm, and five different diameter models of vortex chambers were designed on the original basis. The diameters of the vortex chambers were 40 mm, 45 mm, 55 mm, 60 mm, and 65 mm.

The fluid transfer efficiency obtained by different models is shown in Fig. 12 and Table 2. As the diameter of the vortex chamber increases, there is no significant trend in the efficiency of the pumped fluid be the VCP, with a fluctuation range of 14.36 % to 17.67 %. The VCP model with a diameter of 45 mm has the lowest efficiency, and it has the highest efficiency when the vortex chamber diameter is 50 mm. The diameter has a significant impact on VCP efficiency between 40 mm and 50 mm. The diameter of the vortex chamber has a small impact between 55 mm–65 mm, with a fluctuation range of 15.29 % to 16.78 %.

Table 2 – Parameters of the VCP with different vortex chamber diameters

Diameter	1 (40 mm)	2 (45 mm)	3 (50 mm)	4 (55 mm)	5 (60 mm)
Axial inlet velocity	10.5	9.5	10	10.7	9.8
m_{in}/m_s	0.34	0.31	0.35	0.34	0.34
Efficiency	17.3	14.4	17.7	16.5	16.8

Fig. 13 shows boundary conditions for calculation of solid particle trajectories.

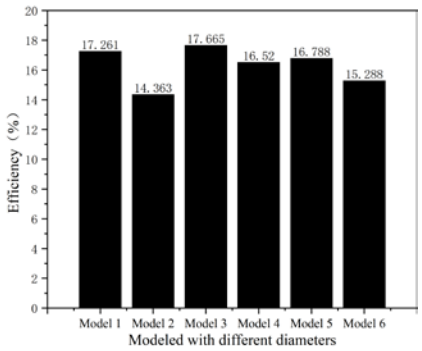

Fig. 12. Efficiency of different VCP models

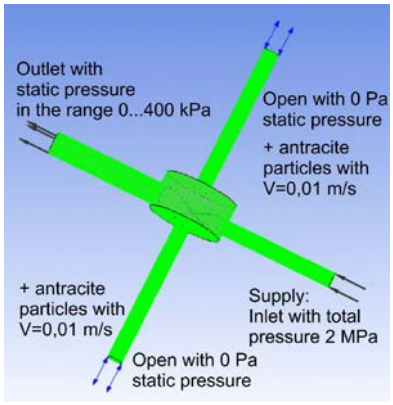

Fig. 13. The boundary conditions for pumping the coal

The mass flow rate of the abrasive medium also determines the different concentrations of solid particles in the VCP. In addition to coal, research has also been conducted on materials such as sand, magnetite, and organic abrasive media. Due to the expansion of different active forces, the trajectory and wear mode are almost identical, only the degree of wear and trajectory are different, so no calculation results are given for these materials.

Compared with turbochargers with mechanical moving bodies, the improvement of the service life [21, 22] of jet pumps depends on many factors such as the concentration of solid particles, the type of wall and particle material, flow rate, and wall thickness. But if there is sufficient wall thickness, the reliability of the jet supercharger is unconditionally higher. To determine the maximum wear area, motion simulations were conducted on coal particles of different sizes ranging from $d_p = 1\times10^{-4}m$ to $d_p = 15\times10^{-4}m$. From Fig. 14, the wear of the vortex chamber wall depends on the diameter of the coal entering the vortex chamber. For coal with different diameters in the vortex chamber, the erosion rate density and averaged volume fraction are shown in Fig. 15 and 16.

Fig. 17 and 18 show that the wear of the vortex chamber wall depends on the mass flow rate of coal entering the vortex chamber. Uniform wear was observed for all flow velocity values and solid particle concentration values, which was also confirmed by calculations of vortex chambers in other devices [23, 24]. This indicates that it is sufficient to increase the thickness of the vortex chamber wall to increase the reliability and durability of devices with vortex chambers, especially VCP.

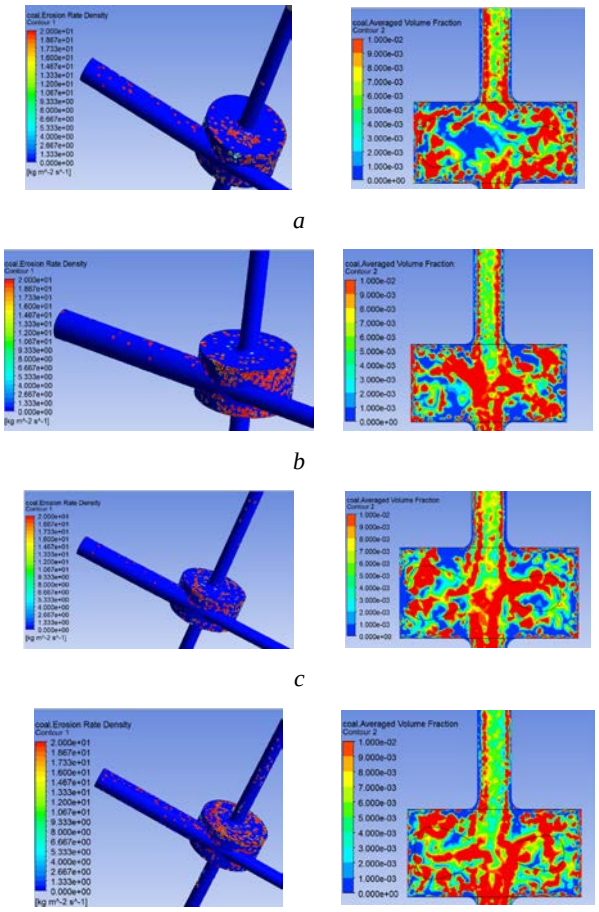

a

b

c

d

Fig. 14. Characteristics of coal movement and erosion in the vortex chamber:
a – diameter of the particles 1.5 mm; *b* – 1 mm; *c* – 0.5 mm; *d* – 0.1 mm

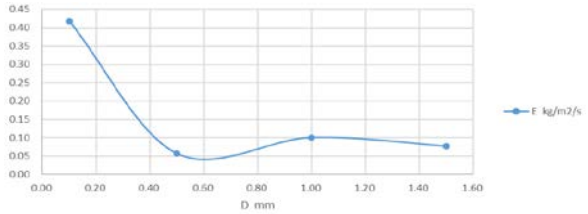

Fig. 15. Dependence of the erosion rate density on solid particles diameter

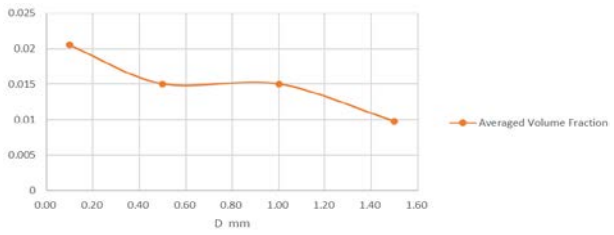

Fig. 16. Dependence of the averaged volume fraction of solid on solid particles diameter

The smaller the particle diameter of the coal, the larger the erosion rate density and mean volume fraction in the vortex chamber. Thus, an increase in particle size should be sought, which will result in less wear. The wear of the pump vortex chamber wall depends on the mass flow rate of coal entering the vortex chamber [25]. The larger the mass flow rate of the abrasive medium, the greater the erosion rate density and the mean volume fraction in the vortex chamber of the VCP.

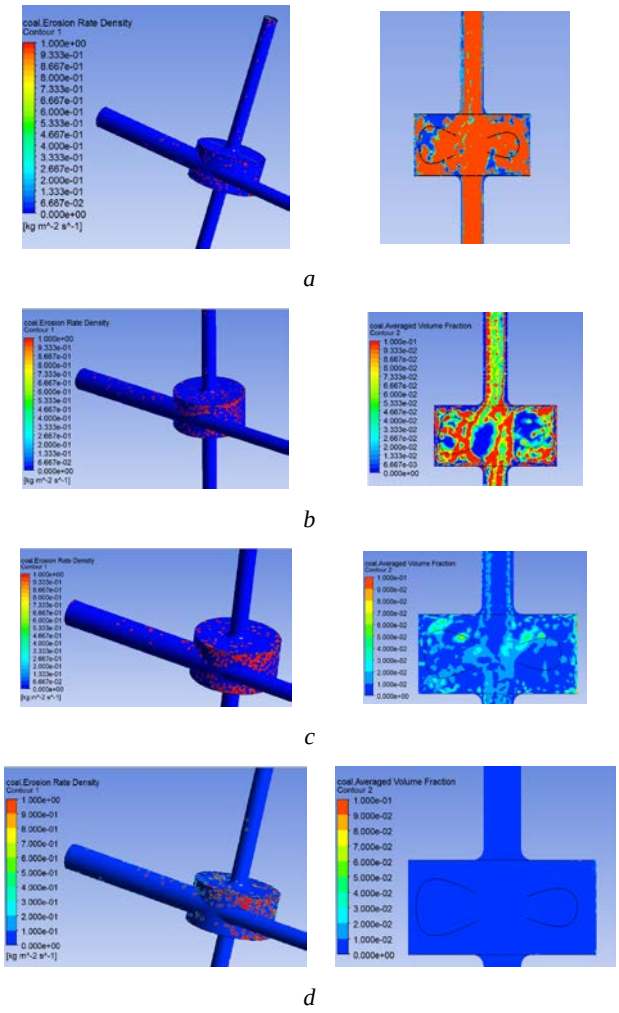

a

b

c

d

Fig. 17. The erosion rate and volume fraction at the different mass flow rates of the coal:
a – 1 kg/s; *b* – 0.1 kg/s; *c* – 0.01 kg/s; *d* – 0.001 kg/s

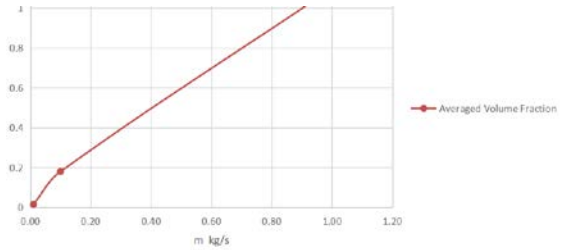

Fig. 18. Dependence of the averaged volume fraction of solid on solid particles flow rate

Conclusions. The vortex chamber pump combines the positive characteristics of the centrifugal pump and the jet pump, and its efficiency is much higher than that of the classical jet pump. This pump differs from the vortex injector by having the pump flow into the tangential outlet channel, which is not available in the vortex injector.

We improved the performance of the vortex chamber pump when pumping water, optimized the angle between tangential channels and the diameter of the vortex chamber, established patterns of coal particles in water,

and determined the wear characteristics of the vortex chamber.

Based on solving the Reynolds equations for water flow, the influence of the angle between the tangential channels of the pump on the energy characteristics is analyzed: an increase in the angle to 180° leads to a decrease in the relative efficiency by 30 %, the outlet pressure by 12 %, and the suction flow rate by 14 %. Thus, the design with a zero angle between the tangential active medium inlet and the tangential outlet channels is optimal in terms of energy-saving pumping performance.

As the diameter of the vortex chamber increases, there is no significant trend in the efficiency of the pumped fluid be the VCP, with a fluctuation range of 14.36 % to 17.67 %.

CRediT authorship contribution statement:

Rogovyi Andrii: Conceptualization, Methodology, Supervision, Investigation;

Ren Qingsheng: Investigation of the solid particles trajectories, Writing – original draft, Visualization, Resources, CFD Software;

Wang Xingrong: Investigation, Writing – original draft, Visualization, Resources, CFD Software;

Neskorozhenyi Artem: Formal analysis, Data curation;

Timchenko Yevhen: Data curation, Writing – review & editing.

References

1. Роговий А. С. *Розробка теорії та методів розрахунку вихорокамерних нагнітачів: дис. ... д-ра техн. наук: 05.05.17.* Харків, 2017. 364 с.
2. Kunii D., Levenspiel O. *Fluidization engineering*. Butterworth-Heinemann, 1991. 491 p.
3. Peng G., Huang X., Zhou L., Zhou G., Zhou H. Solid-liquid two-phase flow and wear analysis in a large-scale centrifugal slurry pump. *Engineering Failure Analysis*. 2020. Vol. 114. P. 104602.
4. Фатєєва Н. М., Шевченко Н. Г., Фатєєв О. М. Надійність гідропневмоагрегатів металорізального устаткування. *Bulletin of the National Technical University "KhPI". Series: Hydraulic machines and hydraulic units.* Kharkiv: NTU "KhPI". 2016. No. 41 (1213). P. 84–87.
5. El-Emam M. A., Zhou L., Yasser E., Bai L., Shi W. Computational methods of erosion wear in centrifugal pump: A state-of-the-art review. *Archives of Computational Methods in Engineering*. 2022. Vol. 29. P. 3789–3814.
6. Сьомін Д. О., Роговий А. С. Вплив умов входу середовища, що перекачується, на енергетичні характеристики вихрекамерних насосів. *Bulletin of the National Technical University "KhPI". Series: Hydraulic machines and hydraulic units.* Kharkiv: NTU "KhPI". 2015. No. 3 (1112). P. 130–136.
7. Роговий А. С. Концепція створення вихорокамерних нагнітачів та принципи побудови систем на їх основі. *Вісник Східноукраїнського національного університету імені Володимира Даля*. Сєвєродонецьк: Вид-во СНУ ім. Володимира Даля. 2017. № 3 (233). С. 168–173.
8. Rogovyi A., Korohodskyi V., Neskorozhenyi A., Hrechka I., Khovanskyi S. Reduction of Granular Material Losses in a Vortex Chamber Supercharger Drainage Channel. *Advances in Design, Simulation and Manufacturing V: Proc. of the 5th Int. Conf. on Design, Simulation, Manufacturing: The Innovation Exchange, DSMIE-2022. Vol. 2: Mechanical and Chemical Engineering (7–10 June 2022, Poznan, Poland)*. Cham: Springer, 2022. P. 218–226.
9. Merzliakov I., Pavlenko I., Chekh O., Sharapov S., Ivanov V. Mathematical modeling of operating process and technological features for designing the vortex type liquid-vapor jet apparatus. *Advances in Design, Simulation and Manufacturing II: Proc. of the 2nd Int. Conf. on Design, Simulation, Manufacturing: The Innovation Exchange, DSMIE-2019 (11–14 June 2019, Lutsk, Ukraine)*. Cham: Springer, 2020. P. 613–622.
10. Levchenko D., Meleychuk S., Arseniev V. Regime characteristics of vacuum unit with a vortex ejector stage with different geometry of its flow path. *Procedia Engineering*. 2012. Vol. 39. P. 28–34.
11. Chu K. W., Kuang S. B., Yu A. B., Vince A., Barnett G. D., Barnett P. J. Prediction of wear and its effect on the multiphase flow and separation performance of dense medium cyclone. *Minerals Engineering*. 2014. Vol. 56. P. 91–101.
12. Sedrez T. A., Decker R. K., da Silva M. K., Noriler D., Meier H. F. Experiments and CFD-based erosion modeling for gas-solids flow in cyclones. *Powder technology*. 2017. Vol. 311. P. 120–131.
13. Sommerfeld M., Sgrott Jr O. L., Taborda M. A., Koullapis P., Bauer K., Kassinos S. Analysis of flow field and turbulence predictions in a lung model applying RANS and implications for particle deposition. *European Journal of Pharmaceutical Sciences*. 2021. Vol. 166. P. 105959.
14. Smirnov P. E., Menter F. R. Sensitization of the SST turbulence model to rotation and curvature by applying the Spalart-Shur correction term. *Journal of Turbomachinery*. 2009. Vol. 131, issue 4. P. 1–8. doi: 10.1115/1.3070573
15. Rezvaya K., Cherkashenko M., Drankovskiy V., Tynyanova I., Makarov V. Using mathematical modeling for determination the optimal geometric parameters of a pump-turbine water passage. *2020 IEEE 4th International Conference on Intelligent Energy and Power Systems (IEPS) (2020, Istanbul)*. Istanbul, 2020. P. 212–216. doi: 10.1109/IEPS51250.2020.9263139
16. Rogovyi A., Shudryk O., Tulska A., Basova Y., Rezvaya K., Makarov V., Machado J. Using modern mechanical design methods for determining the main characteristics of a cryogenic centrifugal pump. *International Journal of Mechatronics and Applied Mechanics*. 2023. Vol. 13. P. 198–208.
17. Rezvaya K., Krupa E., Shudryk A., Drankovskiy V., Makarov V. Solving the hydrodynamical tasks using CFD programs. *2018 IEEE 3rd International Conference on Intelligent Energy and Power Systems (IEPS) (2018, Kharkiv)*. Kharkiv: IEEE, 2018. P. 205–209. doi: 10.1109/IEPS.2018.8559548
18. Pan Y., Spijker C., Raupenstrauch H. CFD modeling of particle dispersion behavior in the MIKE 3 apparatus. *Alexandria engineering journal*. 2022. Vol. 61, issue 12. P. 9305–9313.
19. Peng W., Cao X. Numerical simulation of solid particle erosion in pipe bends for liquid–solid flow. *Powder technology*. 2016. Vol. 294. P. 266–279.
20. Greifzu F., Kratzsch C., Forgber T., Lindner F., Schwarze R. Assessment of particle-tracking models for dispersed particle-laden flows implemented in OpenFOAM and ANSYS FLUENT. *Engineering Applications of Computational Fluid Mechanics*. 2016. Vol. 10, issue 1. P. 30–43.
21. Berladir K., Hovorun T., Gusak O. Strengthening of the NKV type centrifugal pump's shaft by chemical-thermocycling treatment. *Advances in Design, Simulation and Manufacturing IV: Proc. of the 4th Int. Conf. on Design, Simulation, Manufacturing: The Innovation Exchange, DSMIE-2021. Vol. 1: Manufacturing and Materials Engineering (8–11 June 2021, Lviv, Ukraine)*. Cham: Springer, 2021. P. 525–535.
22. Фатєєва Н. М., Фатєєв О. М. Оцінка показників надійності гідроустаткування з урахуванням впливу величини робочого тиску. *Bulletin of the National Technical University "KhPI". Series: Hydraulic machines and hydraulic units.* Kharkiv: NTU "KhPI". 2019. No. 1. P. 104–108. doi: 10.20998/2411-3441.2019.17.15
23. Duarte C. A. R., de Souza F. J., dos Santos V. F. Mitigating elbow erosion with a vortex chamber. *Powder Technology*. 2016. Vol. 288. P. 6–25.
24. Xiao F., Luo M., Huang F., Zhou M., An J., Kuang S., Yu A. CFD–DEM investigation of gas-solid flow and wall erosion of vortex elbows conveying coarse particles. *Powder Technology*. 2023. Vol. 424. P. 118524.
25. Bandi S., Banka J., Kumar A., Rai A. K. Effects of sediment properties on abrasive erosion of a centrifugal pump. *Chemical Engineering Science*. 2023. Vol. 277. P. 118873.

References (transliterated)

1. Rogovyi A. S. *Rozrobka teoriyi ta metodiv rozrakhunku vykhorokamernykh nahnitachiv: dys. ... d-ra tekhn. nauk 05.05.17* [Development of the theory and designing methods of vortex chamber superchargers. Dr. eng. sci. diss.]. Kharkiv, 2017. 364 p.
2. Kunii D., Levenspiel O. *Fluidization engineering*. Butterworth-Heinemann Publ., 1991. 491 p.
3. Peng G., Huang X., Zhou L., Zhou G., Zhou H. Solid-liquid two-phase flow and wear analysis in a large-scale centrifugal slurry

pump. *Engineering Failure Analysis*. 2020, vol. 114, p. 104602.
4. Fatieieva N. M., Shevchenko N. H., Fatyeyev O. M. Nadiynist' hidropnevmoahrehativ metalorizal'noho ustatkuvannya [Reliability of the hydraulic and pneumatic aggregates of the metal cutting equipment]. *Bulletin of the National Technical University "KhPI". Series: Hydraulic machines and hydraulic units.* Kharkiv, NTU "KhPI" Publ., 2016, no. 41 (1213), pp. 84–87.
5. El-Emam M. A., Zhou L., Yasser E., Bai L., Shi W. Computational methods of erosion wear in centrifugal pump: A state-of-the-art review. *Archives of Computational Methods in Engineering*. 2022, vol. 29, pp. 3789–3814.
6. Syomin D. O., Rogovyi A. S. Vplyv umov vkhodu seredovyshcha, shcho perekachuyet'sya, na enerhetychni kharakterystyky vykhrekamernykh nasosiv [The influence of the inlet conditions of the pumped medium on the energy characteristics of vortex chamber pumps]. *Bulletin of the National Technical University "KhPI". Series: Hydraulic machines and hydraulic units.* Kharkiv, NTU "KhPI" Publ., 2015, no. 3 (1112), pp. 130–136.
7. Rogovyi A. S. Kontseptsiya stvorennya vykhorokamernykh nahnitachiv ta pryntsypy pobudovy system na yikh osnovi [The concept of vortex chamber superchargers creation and the principle of systems designing on their basis]. *Visnyk Skhidnoukrayins'koho natsional'noho universytetu imeni Volodymyra Dalya* [Visnik of the Volodymyr Dahl East Ukrainian national university]. Severodonetsk, SNU named after Volodymyr Dahl Publ., 2017, no. 3 (233), pp. 168–173.
8. Rogovyi A., Korohodskyi V., Neskorozhenyi A., Hrechka I., Khovanskyi S. Reduction of Granular Material Losses in a Vortex Chamber Supercharger Drainage Channel. *Advances in Design, Simulation and Manufacturing V: Proc. of the 5th Int. Conf. on Design, Simulation, Manufacturing: The Innovation Exchange, DSMIE-2022. Vol. 2: Mechanical and Chemical Engineering (7–10 June 2022, Poznan, Poland)*. Cham, Springer Publ., 2022, pp. 218–226.
9. Merzliakov I., Pavlenko I., Chekh O., Sharapov S., Ivanov V. Mathematical modeling of operating process and technological features for designing the vortex type liquid-vapor jet apparatus. *Advances in Design, Simulation and Manufacturing II: Proc. of the 2nd Int. Conf. on Design, Simulation, Manufacturing: The Innovation Exchange, DSMIE-2019 (11–14 June 2019, Lutsk, Ukraine)*. Cham, Springer Publ., 2020, pp. 613–622.
10. Levchenko D., Meleychuk S., Arseniev V. Regime characteristics of vacuum unit with a vortex ejector stage with different geometry of its flow path. *Procedia Engineering*. 2012, vol. 39, pp. 28–34.
11. Chu K. W., Kuang S. B., Yu A. B., Vince A., Barnett G. D., Barnett P. J. Prediction of wear and its effect on the multiphase flow and separation performance of dense medium cyclone. *Minerals Engineering*. 2014, vol. 56, pp. 91–101.
12. Sedrez T. A., Decker R. K., da Silva M. K., Noriler D., Meier H. F. Experiments and CFD-based erosion modeling for gas-solids flow in cyclones. *Powder technology*. 2017, vol. 311, pp. 120–131.
13. Sommerfeld M., Sgrott Jr O. L., Taborda M. A., Koullapis P., Bauer K., Kassinos S. Analysis of flow field and turbulence predictions in a lung model applying RANS and implications for particle deposition. *European Journal of Pharmaceutical Sciences*. 2021, vol. 166, p. 105959.
14. Smirnov P. E., Menter F. R. Sensitization of the SST turbulence model to rotation and curvature by applying the Spalart–Shur correction term. *Journal of Turbomachinery*. 2009, vol. 131, issue 4, pp. 1–8. doi: 10.1115/1.3070573
15. Rezvaya K., Cherkashenko M., Drankovskiy V., Tynyanova I., Makarov V. Using mathematical modeling for determination the optimal geometric parameters of a pump-turbine water passage. *2020 IEEE 4th International Conference on Intelligent Energy and Power Systems (IEPS) (2020, Istanbul)*. Istanbul, 2020, pp. 212–216. doi: 10.1109/IEPS51250.2020.9263139
16. Rogovyi A., Shudryk O., Tulska A., Basova Y., Rezvaya K., Makarov V., Machado J. Using modern mechanical design methods for determining the main characteristics of a cryogenic centrifugal pump. *International Journal of Mechatronics and Applied Mechanics*. 2023, vol. 13, pp. 198–208.
17. Rezvaya K., Krupa E., Shudryk A., Drankovskiy V., Makarov V. Solving the hydrodynamical tasks using CFD programs. *2018 IEEE 3rd International Conference on Intelligent Energy and Power Systems (IEPS) (2018, Kharkiv)*. Kharkiv, IEEE Publ., 2018, pp. 205–209. doi: 10.1109/IEPS.2018.8559548
18. Pan Y., Spijker C., Raupenstrauch H. CFD modeling of particle dispersion behavior in the MIKE 3 apparatus. *Alexandria engineering journal*. 2022, vol. 61, issue 12, pp. 9305–9313.
19. Peng W., Cao X. Numerical simulation of solid particle erosion in pipe bends for liquid–solid flow. *Powder technology*. 2016, vol. 294, pp. 266–279.
20. Greifzu F., Kratzsch C., Forgber T., Lindner F., Schwarze R. Assessment of particle-tracking models for dispersed particle-laden flows implemented in OpenFOAM and ANSYS FLUENT. *Engineering Applications of Computational Fluid Mechanics*. 2016, vol. 10, issue 1, pp. 30–43.
21. Berladir K., Hovorun T., Gusak O. Strengthening of the NKV type centrifugal pump's shaft by chemical-thermocycling treatment. *Advances in Design, Simulation and Manufacturing IV: Proc. of the 4th Int. Conf. on Design, Simulation, Manufacturing: The Innovation Exchange, DSMIE-2021. Vol. 1: Manufacturing and Materials Engineering (8–11 June 2021, Lviv, Ukraine)*. Cham, Springer Publ., 2021, pp. 525–535.
22. Fatieieva N. M., Fatyeyev O. M. Otsinka pokaznykiv nadiynosti hidroustatkuvannya z urakhuvannyam vplyvu velychyny robochoho tysku [Estimation of indicators of reliability of hydraulic equipment taking into account the influence of the value of working pressure]. *Bulletin of the National Technical University "KhPI". Series: Hydraulic machines and hydraulic units.* Kharkiv, NTU "KhPI" Publ., 2019, no. 1, pp. 104–108. doi: 10.20998/2411-3441.2019.17.15
23. Duarte C. A. R., de Souza F. J., dos Santos V. F. Mitigating elbow erosion with a vortex chamber. *Powder Technology*. 2016, vol. 288, pp. 6–25.
24. Xiao F., Luo M., Huang F., Zhou M., An J., Kuang S., Yu A. CFD–DEM investigation of gas-solid flow and wall erosion of vortex elbows conveying coarse particles. *Powder Technology*. 2023, vol. 424, p. 118524.
25. Bandi S., Banka J., Kumar A., Rai A. K. Effects of sediment properties on abrasive erosion of a centrifugal pump. *Chemical Engineering Science*. 2023, vol. 277, p. 118873.

Received 12.12.2023

Відомості про авторів / About the Authors

Роговий Андрій Сергійович (***Rogovyi Andrii***) – доктор технічних наук, професор, Національний технічний університет «Харківський політехнічний інститут», завідувач кафедри «Гідравлічні машини ім. Г. Ф. Проскури»; м. Харків, Україна; ORCID: https://orcid.org/0000-0002-6057-4845; e-mail: asrogovoy@ukr.net

Рень Ціншен (***Ren Qingsheng***) – Національний технічний університет «Харківський політехнічний інститут», студент кафедри «Гідравлічні машини ім. Г. Ф. Проскури»; м. Харків, Україна; email: ren.qingsheng@mit.khpi.edu.ua

Ван Сінрун (***Wang Xingrong***) – Національний технічний університет «Харківський політехнічний інститут», студент кафедри «Гідравлічні машини ім. Г. Ф. Проскури»; м. Харків, Україна; email: wang.xingrong@mit.khpi.edu.ua

Нескороженій Артем Олегович (***Neskorozhenyi Artem***) – Харківський національний автомобільно-дорожній університет, аспірант кафедри «Деталі машин і теорії механізмів і машин»; м. Харків, Україна; e-mail: nao@m-impex.com.ua

Тімченко Євген Ігорович (***Timchenko Yevhen***) – Національний технічний університет «Харківський політехнічний інститут», аспірант кафедри «Гідравлічні машини ім. Г. Ф. Проскури»; м. Харків, Україна; e-mail: yevhen.timchenko@mit.khpi.edu.ua